

# Susceptible-Infected-Recovered model on Euclidean network

Abdul Khaleque<sup>1,\*</sup> and Parongama Sen<sup>1,†</sup>

<sup>1</sup>*Department of Physics, University of Calcutta, 92 APC Road, Kolkata 700009, India*

We consider the Susceptible-Infected-Recovered (SIR) epidemic model on a Euclidean network in one dimension in which nodes at a distance  $l$  are connected with probability  $P(l) \propto l^{-\delta}$  in addition to nearest neighbors. The topology of the network changes as  $\delta$  is varied and its effect on the SIR model is studied.  $R(t)$ , the recovered fraction of population up to time  $t$ , and  $\tau$ , the total duration of the epidemic are calculated for different values of the infection probability  $q$  and  $\delta$ . A threshold behavior is observed for all  $\delta$  up to  $\delta \approx 2.0$ ; above the threshold value  $q = q_c$ , the saturation value  $R_{sat}$  attains a finite value. Both  $R_{sat}$  and  $\tau$  show scaling behavior in a finite system of size  $N$ ;  $R_{sat} \sim N^{-\beta/\bar{\nu}} g_1[(q - q_c)N^{1/\bar{\nu}}]$  and  $\tau \sim N^{\mu/\bar{\nu}} g_2[(q - q_c)N^{1/\bar{\nu}}]$ .  $q_c$  is constant for  $0 < \delta < 1$  and increases with  $\delta$  for  $1 < \delta \lesssim 2$ . Mean field behavior is seen up to  $\delta \approx 1.3$ ; weak dependence on  $\delta$  is observed beyond this value of  $\delta$ . The distribution of the outbreak sizes is also estimated and found to be unimodal for  $q < q_c$  and bimodal for  $q > q_c$ . The results are compared to static percolation phenomena and also to mean field results for finite systems. Discussions on the properties of the Euclidean network are made in the light of the present results.

PACS numbers: 64.60.Cn, 64.60.aq, 64.60.F-, 64.60.ah

## I. INTRODUCTION

Studies of familiar static and dynamic phenomena on complex networks have led to some surprises [1–3] in recent times. For example, the Ising model which in one dimension does not have a phase transition, showed not only the existence of a phase transition but also that it occurs with mean field criticality [2, 4–7] on the Watts-Strogatz (WS) [8] type network. On the scale-free network also, it showed a behavior not encountered usually on regular lattices; the transition temperature showed a logarithmic increase with the system size [9]. Among the well studied dynamical phenomena on networks [3] are opinion dynamics models [10], disease and damage propagation [11–14], synchronization of coupled oscillations [2, 15], zero temperature quench of Ising and other spin models [16–20], etc. Just like the static results on networks, there have been special features of the dynamical phenomena as well. On complex networks, zero temperature quenching of Ising model shows freezing even in a one dimensional network with additional random links. Another example is the voter model: its dynamics can be conceived in different manners on networks leading to the conservation of different physical quantities. However, on regular lattices these different dynamical rules are equivalent [10].

A standard model for epidemic spreading is the Susceptible-Infected-Recovered (SIR) model where individuals can be in three possible states; susceptible: who are liable to be infected, recovered: those who contracted the disease but are now recovered and immunized, infected: people who are suffering from the disease and can infect others. A very well known result for the SIR

model is that it is like a dynamical percolation problem and its critical behavior coincides with that of static isotropic percolation on regular lattices [21]. On the other hand, another model for disease spreading, namely the Susceptible-Infected-Susceptible (SIS) is identical to a directed percolation problem. Percolation phenomena has also been studied extensively on complex networks (earliest works appear in [22–24] and comprehensive reviews are available in [2, 3]) and it is possible to compare the two phenomena of epidemic spreading and percolation on complex networks as well.

Although extensive research work on epidemic spreading on scale free and WS networks have been made, it may be noted that social connections are neither scale free nor like those considered in the WS network. In fact, many social networks have a spatial dependence in the connection probability of the nodes [25]. We thus consider SIR on a spatial model in which random long range links between nodes at a Euclidean distance  $l$  are added with probability  $P(l) \propto l^{-\delta}$ . Nearest neighbor links are always present in this model. In [26, 27], a similar model in two dimensions was considered, but the probability  $P(l)$  was essentially dictated by the heterogeneity of the degree distribution, and only short range links followed the power law distribution while long range links were added randomly.

Static properties of the network considered in this paper are quite well studied [28, 29]. The network behaves as a small world network for  $\delta < 1$  and as a regular one dimensional lattice for  $\delta > 2$ . Some ambiguities remain regarding its behavior when  $1 < \delta < 2$ . While some results suggest the network is still a small world here, other works claim that it has a finite lattice-like behavior. Dynamic phenomena like zero temperature coarsening of Ising model and searching have also been studied on this network [20, 30].

The aim is to locate the infection threshold values as a function of  $\delta$  and find out the critical behavior for SIR

\*Email: 7187ak@gmail.com

†Email: pspthy@caluniv.ac.in

on the Euclidean network. This may also help in understanding the nature of the network in the controversial region  $1 < \delta < 2$  by considering a dynamical process. We have also studied the way the recovered fraction grows in time as well as the total duration of the entire epidemic spreading process.

In section II, we describe the model and method briefly and follow it up with the results in section III. In section IV, we discuss a simple model (mean field type) to make some comparisons. In section V, the results are discussed and compared to earlier studies made on the same network. In the last section concluding remarks are made.

## II. MODEL AND METHODS

The network is generated in the following way: in a system of  $N$  nodes placed on the sites of a one dimensional lattice, all nearest neighbors are first connected. Additional long range links (one per node on an average) are established at a distance  $l > 1$ . This is done in the following way: two nodes are selected randomly; if they are not connected already, a connection is established with a probability  $P(l) \propto l^{-\delta}$  ( $l$  is the distance separating the nodes). The process is stopped as soon as  $N/2$  links have been formed this way. The average degree of the nodes is therefore three.

In a homogeneous system, the SIR model can be described in terms of the densities of susceptible, infected and recovered nodes,  $S(t)$ ,  $I(t)$  and  $R(t)$ , respectively, as function of time. These three densities are related through the normalization condition:

$$S(t) + I(t) + R(t) = 1, \quad (1)$$

and they obey the following system of differential equations [31]:

$$\frac{dS}{dt} = -q(k-1)IS, \quad (2)$$

$$\frac{dI}{dt} = -\mu I + q(k-1)IS, \quad (3)$$

$$\frac{dR}{dt} = \mu I. \quad (4)$$

These equations can be interpreted as follows: infected nodes become recovered at a rate  $\mu$ , while susceptible nodes become infected at a rate proportional to both the densities of infected and susceptible nodes. Here,  $q$  is the infection rate and  $k$  is the number of contacts per unit time.

In the simulation, systems with size  $N < 2^{14}$  have been taken. Time is discretized and only the infection rate  $q$  is used as a parameter; infected people recover within one unit of time and can infect susceptible individuals with probability  $q$  connected directly to them within the same time scale. Initially all nodes are susceptible, one arbitrary node is chosen and taken to be infected. For the same network, 600 such choices have been taken and

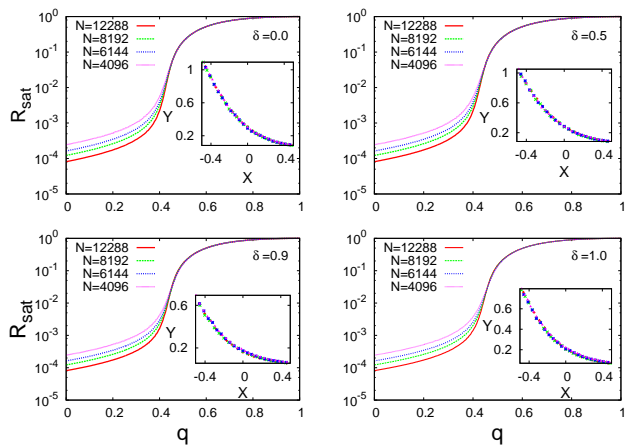


FIG. 1: (Color online) Variation of  $R_{sat}$  with  $q$  for different values of  $\delta = 0.0, 0.5, 0.9$  and  $1.0$ . Insets show the data collapse where  $Y = R_{sat}N^{\beta/\bar{\nu}}$  has been plotted against  $X = (q - q_c)N^{1/\bar{\nu}}$ .

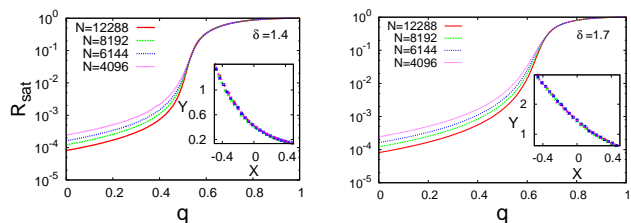


FIG. 2: (Color online) Variation of  $R_{sat}$  with  $q$  for different values of  $\delta = 1.4$  and  $1.7$ . Insets show the data collapse where  $Y = R_{sat}N^{\beta/\bar{\nu}}$  has been plotted against  $X = (q - q_c)N^{1/\bar{\nu}}$ .

quantities are averaged. A secondary averaging is made by considering 100 different network configurations. Dynamics takes place in parallel; all the individuals revise their epidemiological state in one time step. Periodic boundary condition has been used in the simulation.

## III. RESULTS

### A. Static results

#### 1. Fraction of recovered population

We calculate the fraction  $R(t)$  of recovered nodes as a function of time. This means the total fraction of nodes who are recovered till the time of measurement. It is also identical to the fraction of the population who have been infected at some point of time in the past.  $R(t)$  reaches a saturation value  $R_{sat} < 1$  which depends on both  $q$  and  $\delta$ . We use synchronous dynamics to update the state of the nodes. The total duration  $\tau$  of the epidemic is also estimated.

As a function of the infection probability  $q$ ,  $R_{sat}$  is plotted for different values of  $\delta$  (Fig. 1). From the knowledge that SIR shows the same criticality as the isotropic

percolation problem, it can be expected that a continuous phase transition takes place here. Since it is a finite size system, one can use the conventional finite size scaling method to estimate the critical (threshold) value  $q_c$  and the associated critical exponents.  $R_{sat}$  vanishes below  $q_c$  in the thermodynamic limit and should have a scaling form similar to magnetization. Therefore, the following finite size scaling form for  $R_{sat}$  is used:

$$R_{sat} \propto N^{-\beta/\tilde{\nu}} g_1((q - q_c)N^{1/\tilde{\nu}}), \quad (5)$$

where  $g_1$  is a scaling function. We obtain data collapse with appropriate values of  $\beta$ ,  $q_c$  and  $\tilde{\nu}$  (Fig. 1 insets). Let us first discuss the region  $0 \leq \delta < 1$  where  $q_c \simeq 0.430$  does not show any appreciable dependence on  $\delta$ . For  $\delta = 0$ , the results should be comparable to a (addition type) Watts-Strogatz type network. The percolation threshold is known to be 0.401 there [24]. Our result for  $q_c$  is slightly higher which could be because the average degree is different and also the fact that nearest neighbor links are always present here such that in comparison, long range neighbors are smaller in number.

Results for  $0 \leq \delta < 1$  show that the value of  $\beta \simeq 1$  and  $\tilde{\nu} \simeq 3$  are also unchanged in this region. This is not surprising, this region is known to have a small world behavior. Hence, mean field behavior is expected to be valid here and we find the value exponent  $\beta = 1$  indeed matches with the mean field value for percolation. Assuming  $\tilde{\nu} = \nu d$ , where  $d = 6$  is the upper critical dimension [2, 6, 32, 33], one gets  $\nu = 1/2$  from the fact that  $\tilde{\nu} \simeq 3$ , which also coincides with the mean field value for percolation phenomenon.

For  $\delta > 1$ ,  $q_c$  increases and approaches 1 at a value of  $\delta$  close to 2. This is expected, as for  $\delta > 2.0$ , the network behaves as a regular network in one dimension where  $q_c = 1$ . The value of the exponent  $\tilde{\nu}$  however, appears to be unchanged while  $\beta$  shows a variation with  $\delta$ , although not very strong.  $\beta$  starts deviating from the mean field value at around  $\delta = 1.4$ .

The total duration  $\tau$  also shows a dependence on  $q$ ; its peak value increases with the system size (Fig. 3). This data is also analyzed by finite size scaling assuming the scaling form

$$\tau \propto N^{\mu/\tilde{\nu}} g_2((q - q_c)N^{1/\tilde{\nu}}), \quad (6)$$

where  $g_2$  is another scaling function.  $\tilde{\nu}$  turns out to be very close to 3.0 from the above analysis as well for all  $\delta$  values, while  $\mu$  shows a dependence on  $\delta$  for  $\delta \geq 1.3$ .

We show the values of the threshold values  $q_c$ , and the exponents  $\mu$  and  $\beta$  as functions of  $\delta$  in Fig. 5. Here  $q_c$  shows variation with  $\delta$  for  $\delta > 1.0$ , the values of the exponents start differing from the mean field value at  $\delta > 1.3$ .  $q_c$  appears to reach 1 slightly above  $\delta = 2.0$ , we have checked that for  $\delta = 2.2$ ,  $q_c$  is very close to 1.

If we put  $q = q_c$ , the variation of  $\tau$  with  $N$  shows that it diverges algebraically with  $N$  sublinearly in the entire region  $0 \leq \delta \leq 2$ . This is interesting:  $\tau$  may be regarded as the minimum number of steps connecting two individuals

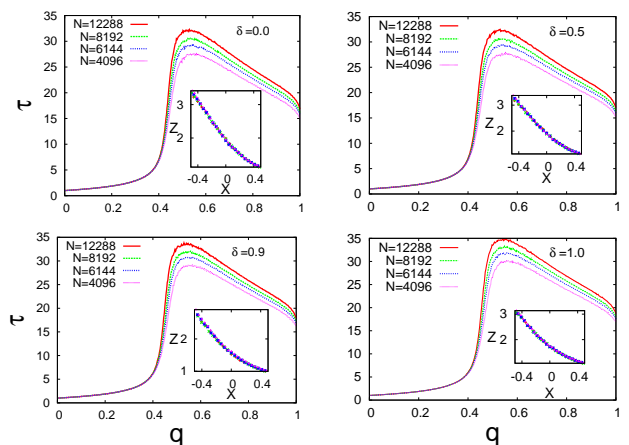


FIG. 3: (Color online) Variation of  $\tau$  with  $q$  for different values of  $\delta = 0.0, 0.5, 0.9$  and  $1.0$ . Insets show the data collapse where  $Z = \tau N^{-\mu/\tilde{\nu}}$  has been plotted against  $X = (q - q_c)N^{1/\tilde{\nu}}$ .

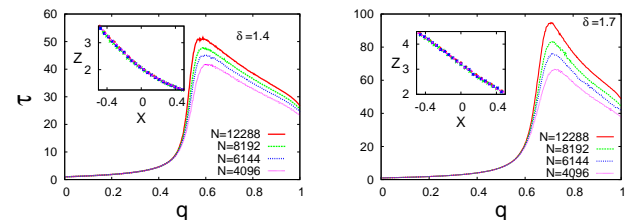


FIG. 4: (Color online) Variation of  $\tau$  with  $q$  for different values of  $\delta = 1.4$  and  $1.7$ . Insets show the data collapse where  $Z = \tau N^{-\mu/\tilde{\nu}}$  has been plotted against  $X = (q - q_c)N^{1/\tilde{\nu}}$ .

for exactly  $q = 1$  in the network, i.e., it is comparable to the diameter of the network. However, one might expect that for  $q \geq q_c$ , when spanning occurs, a finite number of the nodes can be reached by the infection procedure and hence  $\tau$  gives an estimate of the average number of steps connecting two individuals for the entire network (which may not necessarily be the minimum path). We know that in the small world region, the diameter scales as  $\log(N)$  but here we get a different scaling for  $\tau$ . We

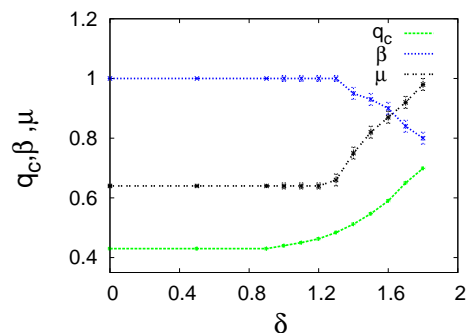


FIG. 5: (Color online) The exponents and the transition point shown against  $\delta$ .

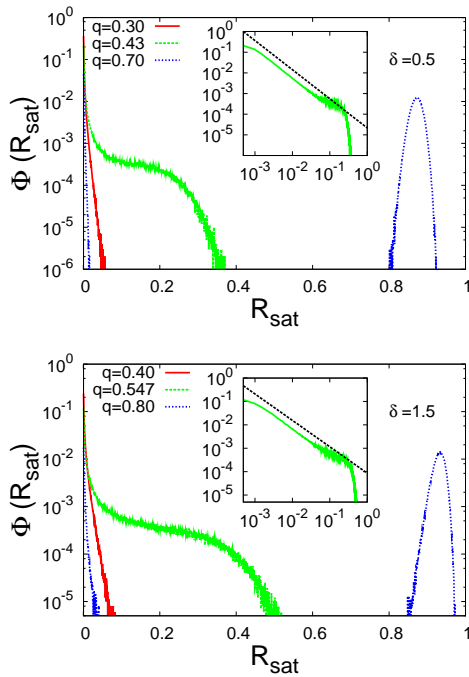


FIG. 6: (Color online) Frequency distributions for outbreak size  $R_{sat}$  are shown for  $N = 2048$  for two values of  $\delta$ . Data for  $q < q_c$ ,  $q > q_c$  and  $q = q_c$  are shown. For  $q < q_c$  the distribution is unimodal while for  $q > q_c$ , it is bimodal with two peaks occurring at  $R_{sat} \sim 1/N$  and  $R_{sat} \sim O(1)$  (see text). Insets show that the data at  $q = q_c$  has a power law variation.

will discuss this point in section IV and V.

## 2. Distribution of the outbreak size

In the discussion in the preceding subsection, results for the average value of the outbreak size  $R_{sat}$  has been reported. We have also studied the distribution  $\Phi(R_{sat})$  of  $R_{sat}$  which shows that it is bimodal in nature for  $q > q_c$  and unimodal for  $q < q_c$  as found in [34, 35].  $\Phi(R_{sat})$  has a peak near  $\frac{1}{N}$  for all values of  $q$  which appears for the cases when the initially infected single node cannot transmit the disease to anyone else. The peak value at  $1/N$  decreases with  $q$  as expected. For  $q > q_c$  the  $\Phi(R_{sat})$  has a secondary peak at a larger value of  $R_{sat} \sim O(1)$  (Fig. 6). It may be noted that the peak values at  $R_{sat} \sim \frac{1}{N}$  and  $R_{sat} \sim O(1)$  are comparable for  $q > q_c$  which makes the average value of  $R_{sat}$  a meaningful quantity. At  $q_c$ ,  $\Phi(R_{sat})$  varies continuously and the tail of  $\Phi(R_{sat})$  has power law decay as shown in the inset of Fig 6. The associated exponent varies with  $\delta$ , for example, it is  $\sim 1.41$  for  $\delta = 0.5$  and  $\sim 1.13$  for  $\delta = 1.5$ .

Such a bimodal behavior of distribution of outbreak sizes, which occurs as a single agent is assumed to be infected initially, is consistent with empirical data of disease spreading analyzed by Watts et al [36].

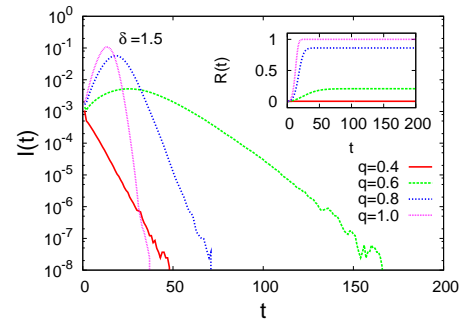


FIG. 7: (Color online) The infected fraction of nodes shown against time for  $\delta = 1.5$  for a system of size  $N = 2048$ . There is a peak at  $t_p$  for  $q > q_c$ . Inset shows the variation of total recovered fraction of nodes with time for  $\delta = 1.5$ .

## B. Dynamical results

The growing density of recovered population  $R(t)$  has been plotted in the inset of Fig. 7. The data shows the expected saturation and a very fast growth at initial times suggesting an exponential behavior at early times [37]. It is found that the numerical data for  $R(t)$  can be fitted to the form:

$$R(t) = \frac{a \exp(t/T)}{1 + c \exp(t/T)} - \frac{a}{1 + c}, \quad (7)$$

where  $a$ ,  $c$  and  $T$  depends on  $q$  and  $\delta$ . The boundary condition assumed in the fitting is  $R(0) = 0$ .

The fraction of nodes infected at time  $t$ ,  $I(t) = R(t + 1) - R(t)$  is plotted in Fig. 7. An initial growth and a peak value occurs at time  $t = t_p$  only for  $q > q_c$ . For  $q < q_c$ , one gets a decaying behaviour right from  $t = 0$ . Such a decaying behaviour can occur if secondary infections are less than primary infections. Hence approximately,

$$(k - 1)^2 q^2 < (k - 1)q \quad (8)$$

which gives

$$q < 1/(k - 1) = q_c. \quad (9)$$

Hence this argument can explain the absence of the peak for  $q < q_c$ . The fact that the recovered population is no longer susceptible has been ignored in this argument, but for initial times, this will not matter when the recovered population is very small. This is supported by the data presented in Fig 6 which show that for  $q < q_c$ ,  $R_{sat}$  has very small values only.

The variation of  $t_p$  against  $q$  shows  $t_p$  increases sharply from zero close to the transition point  $q_c$  (Fig. 8). Thus one can get an independent estimate of  $q_c$  from this study. One may also plot the peak value  $I(t_p)$  as a function of  $q$  which again shows an increase from zero close to the transition point (Fig. 9).

One can check how good is the fitting (eq. 7) by the following approach. Assuming continuous time,  $I(t)$  can

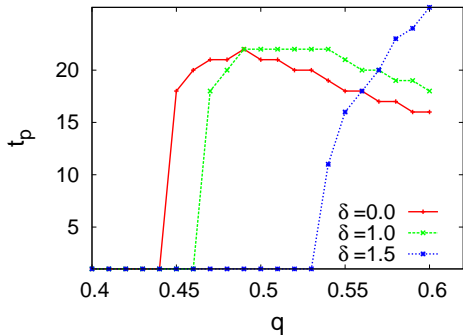


FIG. 8: (Color online) The time  $t_p$  at which the peak value occurs against  $q$  shows a sharp rise near  $q_c$  (Data shown for  $N = 2048$ ).

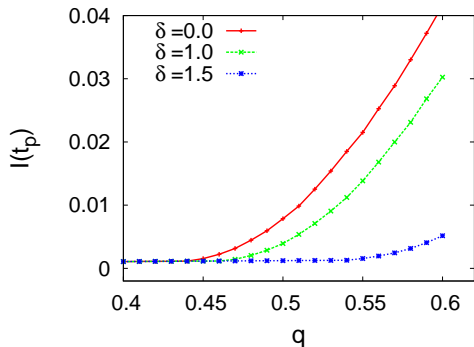


FIG. 9: (Color online) The peak value of  $I$  against  $q$  shows a monotonic increase (Data shown for  $N = 2048$ ).

be expressed as  $\frac{dR}{dt}$ . Let  $F(t) = \frac{dR}{dt}$ , then from eq. (7),

$$F(t) = \frac{\frac{a}{T} \exp(t/T)}{(1 + c \exp(t/T))^2}. \quad (10)$$

At large times,  $F(t)$  should fall exponentially with  $t$ ,  $I(t)$  indeed shows such a behavior. The value of  $t = t_p$  where  $F(t)$  is maximum is found by solving the equation

$$\frac{dF}{dt} = \frac{\frac{a}{T^2} \exp(t/T) - \frac{ac}{T^2} (\exp(t/T))^2}{(1 + c \exp(t/T))^3} = 0, \quad (11)$$

which gives

$$t_p = T \ln \left( \frac{1}{c} \right). \quad (12)$$

At  $t_p = T \ln(\frac{1}{c})$ , the value of  $F(t)$  is

$$F(t_p) = \left( \frac{dR}{dt} \right)_{t_p} = \frac{a}{4cT}. \quad (13)$$

Putting the values of  $a$ ,  $c$  and  $T$  obtained from the fitting,  $t_p$  and  $F(t_p)$  can be computed from eqs (12) and (13) and compared to the actual data. It shows very good agreement showing the quality of the fit. The comparison is shown in Table I for a particular value of  $q$ .

TABLE I:  $a$ ,  $c$  and  $T$  for three values of  $\delta$  and comparison of  $t_p$  and  $F(t_p)$  obtained from fitting and data ( $q = 0.58$ )

$\delta$	$a$ $\times 10^{-3}$	$c$ $\times 10^{-3}$	$T$	$t_p$ (fit)	$t_p$ (data)	$F \times 10^{-3}$ (fit)	$F \times 10^{-3}$ (data)
0.0	3.69	7.95	3.47	16.78	17	33.3	33.0
1.0	5.34	12.8	4.47	19.48	19	23.3	23.1
1.5	19.7	133	11.87	23.95	23	3.12	3.15

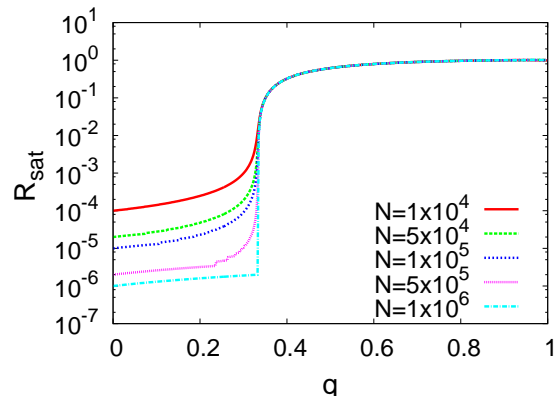


FIG. 10: (Color online) Variation of  $R_{sat}$  with  $q$  for mean field SIR model.

#### IV. MEAN FIELD RESULTS FOR FINITE SIZES

One can formulate a mean field type recursion relation with discrete time steps for the SIR model in which the average degree is  $\langle k \rangle$  from eq. (2),

$$I(t) = q(\langle k \rangle - 1)I(t-1)S(t-1). \quad (14)$$

As  $I(t) = R(t+1) - R(t)$  and  $S = 1 - R - I$ , this gives,

$$R(t+1) - R(t) = q(\langle k \rangle - 1)(R(t) - R(t-1))(1 - R(t)). \quad (15)$$

The initial conditions are  $R(0) = 1/N$  and  $R(1) = R(0) + q\langle k \rangle R(0)(1 - R(0))$ . Obviously, here one assumes that the neighbors to which the infection spreads can be anywhere. We note that the system size enters through the initial conditions only, and it has been assumed that only one individual is infected in the beginning.

$R(t)$  and  $\tau$  are numerically estimated for different sizes using  $\langle k \rangle = 4$  and shown in Figs 10 and 11. The threshold value of  $q$  is very close to the theoretical estimate  $q_c = 1/(\langle k \rangle - 1) = 1/3$  [14].

These data however do not show any finite size scaling behavior, i.e., a data collapse cannot be obtained. This is compatible with the fact that for a mean field model, finite size scaling does not work [38]. For the Euclidean model considered in this paper on the other hand, it is possible to obtain mean field exponents by finite size scaling in a finite region of the parameter space.



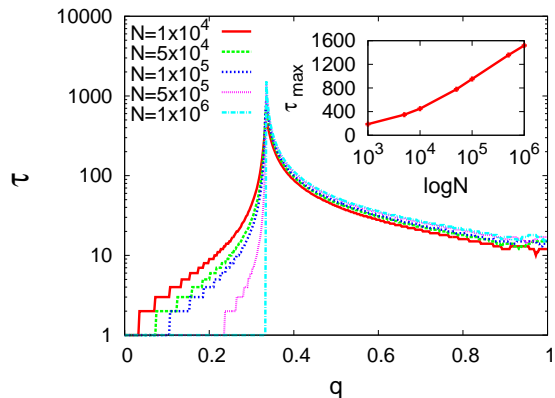


FIG. 11: (Color online) Variation of  $\tau$  with  $q$  for mean field SIR model. Inset shows the behavior of  $\tau_{max}$  with system size for mean field SIR model.

Similarly,  $\tau$  also does not show finite size scaling. But exactly at  $q_c$ , it has a peak value which scales with  $N$  as  $\log(N)$ . This agrees with the result of [39]. Interestingly, such  $\log(N)$  behavior for  $\tau$  is not obtained at  $q = q_c$  for any value of  $\delta$  for the Euclidean network. This is consistent with the earlier results [40, 41] that for small world networks, when percolation is considered, the giant component that emerges does not have a small world geometry.

## V. DISCUSSIONS OF THE RESULTS

Before discussing the results, it is useful to recapitulate briefly the studies already made on this network as comparison with these earlier works is necessary.

### A. Earlier studies on this network: Static properties

It has been mentioned earlier that there are some results available for the static properties of the network. A number of studies have been made to investigate the behavior of the network by calculating numerically the average shortest path as a function of the network size [42–45]. Two earlier works [44, 45] in which the greedy algorithm was used to evaluate the shortest paths, showed contradictory results. The study made with much larger networks indicated that the network had finite dimensional behavior for  $1 \leq \delta < 2$  [45] while in [44], it was claimed that up to  $\delta = 2$ , the small world behavior exists. In a more recent work [29], all possible shortest paths were evaluated numerically using a burning algorithm, and it was again found that the network retains the small world property up to  $\delta = 2$  while the clustering coefficient vanishes below  $\delta = 1$ . Such a result was also obtained in [46]. However, one can still argue that it is an effect of finite sizes [45]. Simple scaling arguments

suggest that there may be two transitions occurring at  $\delta = 1.0$  and  $\delta = 2.0$  [46].

### B. Critical phenomena studied earlier on this network

The Ising model has been studied on the Euclidean network and again in two different studies contradictory results were obtained. While in [32] it was found that the network behaves as a finite dimensional system for  $1 < \delta < 2$ , the study with the larger network [47] indicated a small world behavior up to  $\delta = 2.0$ . Both studies, however, showed that the transition temperature remained  $\delta$  independent up to  $\delta = 1$ .

SIR is expected to be related to percolation phenomena as already mentioned. Percolation has been studied in this type of network recently [48]. The detailed study was made in two dimensions. In one dimension, results for two values of  $\delta = 1.5$  and  $1.75$  showed that the exponents are  $\delta$  dependent. The values of the threshold infection probability turn out to be larger than our results. This is probably because the networks are constructed in slightly different ways and also could be because site percolation was considered in [48].

### C. Present results and comparisons

In comparison, the results obtained in the present work do not apparently lead to any definite conclusions for the behavior of the network for  $1 < \delta < 2$ , while the mean field behavior obtained for  $\delta < 1$  is consistent with the earlier results. In the mean field region, one has to use the upper critical dimension in the scaling relation to extract the exponents just like in the case of Ising model [32].

To analyse the region  $1 < \delta < 2$  carefully, the results for the static exponents  $\tilde{\nu}$  and  $\beta$  may be considered by comparing to the exponent values of isotropic percolation in different dimensions.  $\tilde{\nu}$  remains a constant in this region while  $\beta$  shows a change. It may be possible that  $\tilde{\nu}$  remains constant with both  $\nu$  and  $d$  varying. However, for percolation, we do not have such invariance of  $\nu d$  for dimensions 1-6 [49]. This suggests that the dimensionality is actually not changing.  $\beta$  on the other hand does show a deviation from its mean field value (equal to 1) for  $\delta \geq 1.4$ . However, the deviation is not appreciable; the extrapolated value of  $\beta$  at  $\delta = 2.0$  does not reach anywhere close to zero as it should. Rather, the value of  $\beta$  for  $\delta$  even very close to 2.0 corresponds to what one would expect for a five dimensional lattice which indicates that in all probability it has a constant value up to  $\delta = 2.0$  but shows small changes in finite systems due to the transition occurring at  $\delta = 2.0$ .

One can also consider the dynamic exponent  $\mu$  which shows a stronger dependence on  $\delta$  in the region  $1 < \delta < 2$  compared to  $\beta$ . Here it may be recalled that even in the

small world region,  $\mu$  has a finite indicating  $\tau$  has a power law behaviour while in the finite mean field case,  $\tau$  shows a logarithmic behaviour (sec IV). Hence in contrast to the static exponents,  $\mu$  does not reflect the behaviour of the network even in the small world region. Thus conclusions about the network's properties cannot be made on the basis of the behavior of  $\mu$ .

We have to compare the present results with those of static percolation on the same network which is available in [48]. For the results of the two points reported in this paper, the criticality appears to change appreciably as  $\delta$  varies between 1 and 2 and does not show mean field behavior. The disagreement may be because of several factors: the construction of the two networks and the average degree is different, secondly, it could be that the correspondence between percolation and SIR is not entirely true for the Euclidean network in this region. Such lack of correspondence has been noted in some earlier works [2]. Also, there could be such strong finite size effects that trying to compare results from two different studies is not useful.

## VI. CONCLUDING REMARKS

From the discussion of the last section, we arrive at the following conclusion: SIR on this network shows mean field behavior up to  $\delta = 2.0$  for at least the system sizes considered here. Evidently therefore, the network does not behave as a finite dimensional lattice for the region  $1 < \delta < 2$  as has been claimed in some earlier works but effect of finite sizes are quite strong in the region  $\delta \geq 1.4$ .

Talking about dimensionality, we would like to add a few words here. It is customary to use the upper critical dimension  $d$  and express  $\tilde{\nu} = \nu d$  to get the mean field critical exponents using finite size scaling in these types of systems [2]. Hence one uses  $d = 4$  for the Ising model

and  $d = 6$  for the percolation case. Surely one cannot assign a unique dimensionality to the network in this way at least in the mean field regime. However, assigning a dimension to the network in the mean field region is perhaps meaningless.

What happens when mean field results are no longer valid? Theoretically, it is possible that one extracts a dimensionality in between 4 and 6 (which is what we are getting in the present work if we consider the value of  $\beta$ ) where percolation will not show mean field results but Ising model will. This appears far fetched and compels us to believe that the entire region  $0 < \delta < 2$  has mean field behavior in agreement with [47].

The critical point shows variation with  $\delta$  in the intermediate region as did the transition temperature for the Ising model [32, 47]. Not only that, the time duration also shows appreciable change in the scaling with the system size at criticality here. Apparently, the network having appreciable clustering leads to these changes which is felt in the intermediate region but overall small world property is retained such that mean field behavior prevails.

We move over to a more profound question, do we reach any conclusion about what is the actual behavior of the network for  $1 < \delta < 2$ ? Still this issue is not resolved. As far as Ising model criticality and the SIR process is concerned, the latest results suggest it has a small world behavior. However, results of static percolation and some geometric properties indicate otherwise. The only possible solution to justify these earlier results may be that at finite sizes, the network shows a small world behavior and deviations are only perceptible at very large length scales.

Acknowledgements: The authors thank Arnab Chatterjee for a careful reading of the manuscript. AK acknowledges financial support from UGC sanction no. UGC/534/JRF(RFSMS).

- 
- [1] M. E. J. Newman, *Networks: An Introduction* (Oxford University Press, USA, 2010).
  - [2] S. N. Dorogovtsev and A. V. Goltsev, *Rev. Mod. Phys.* **80**, 1275 (2008) and the references therein.
  - [3] A. Barrat, M. Barthelemy and A. Vespignani, *Dynamical processes on complex networks* (Cambridge University Press, Cambridge, U.K., 2008).
  - [4] A. Barrat and M. Weigt, *Eur. Phys. J. B* **13**, 547 (2000).
  - [5] M. Gitterman, *J. Phys. A* **33**, 8373 (2000).
  - [6] C. P. Herrero, *Phys. Rev. E* **65**, 066110 (2002).
  - [7] H. Hong, B. J. Kim, and M. Y. Choi, *Phys. Rev. E* **66**, 018101 (2002).
  - [8] D. J. Watts and S. H. Strogatz, *Nature* **393**, 440 (1998).
  - [9] C. P. Herrero, *Phys. Rev. E* **69**, 067109 (2004).
  - [10] C. Castellano, S. Fortunato and V. Loreto, *Rev. Mod. Phys.* **81**, 591 (2009) and the references therein.
  - [11] R. Pastor-Satorras and A. Vespignani, *Phys. Rev. Lett.* **86**, 3200 (2001).
  - [12] A. Vazquez, R. Pastor-Satorras, and A. Vespignani, *Phys. Rev. E* **65**, 066130 (2002).
  - [13] M. E. J. Newman, *Phys. Rev. E* **66**, 016128 (2002).
  - [14] Y. Moreno, R. Pastor-Satorras and A. Vespignani, *Eur. Phys. J. B* **26**, 521 (2002).
  - [15] P. M. Gade and C. -K. Hu, *Phys. Rev. E* **62**, 6409 (2000).
  - [16] P. Svenson, *Phys. Rev. E* **64**, 036122 (2001).
  - [17] O. Haggstrom, *Physica A* **310**, 275 (2002).
  - [18] D. Boyer and O. Miramontes, *Phys. Rev. E* **67**, 035102 (2003).
  - [19] P. K. Das and P. Sen, *Eur. Phys. J. B* **47**, 306 (2005).
  - [20] S. Biswas and P. Sen, *Phys. Rev. E* **84**, 066107 (2011).
  - [21] P. Grassberger, *Mathematical Biosciences* **63**, 157 (1983).
  - [22] M. E. J. Newman and D. J. Watts, *Phys. Rev. E* **60**, 7332 (1999).
  - [23] R. Cohen, K. Erez, D. ben-Avraham and S. Havlin, *Phys. Rev. Lett.* **85**, 4626 (2000).
  - [24] C. Moore and M. E. J. Newman, *Phys. Rev. E* **61**, 5678 (2000).

- [25] M. Barthelemy, Phys. Rep. **499**, 1 (2010).
- [26] C. P. Warren, L. M. Sander and I. M. Sokolov, Phys. Rev. E **66**, 056105 (2002).
- [27] L. M. Sander, C. P. Warren and I.M. Sokolov, Physica A **325**, 1 (2003).
- [28] P. Sen in *Recent developments in Theoretical Physics*, eds. S. Ghosh and G. Kar (Platinum Jubilee series of ISI, India) World Scientific (2010) P. 375.
- [29] S. Goswami, S. Biswas and P. Sen, Physica A **390**, 972 (2011).
- [30] H. Zhu and Z-X. Huang, Phys. Rev. E **70**, 036117 (2004).
- [31] J. Marro and R. Dickman, *Nonequilibrium Phase Transitions in Lattice Models* (Cambridge University Press, Cambridge, U.K., 1999)
- [32] A. Chatterjee and P. Sen, Phys. Rev. E **74**, 036109 (2006).
- [33] S. Biswas, A. Chatterjee and P. Sen, Physica A **391**, 3257 (2012).
- [34] D. H. Zanette, Phys. Rev. E **64**, 050901 (2001).
- [35] L. K. Gallos and P. Argyrakis, Physica A **330**, 117 (2003).
- [36] D. J. Watts, R. Muhamad, D. C. Medina and P. S. Dodds, PNAS **102**, 11157 (2005).
- [37] H. W. Hethcote, SIAM Review **42**, 599 (2000).
- [38] E. Brezin, J. Phys. France **43**, 15 (1982).
- [39] E. Ben-Naim and P. L. Krapivsky, Phys. Rev. E **69**, 050901(R) (2004).
- [40] R. Cohen, K. Erez, D. ben-Avraham, and S. Havlin, Phys. Rev. Lett. **86**, 3682 (2001).
- [41] R. Cohen, S. Havlin and D. Ben-Avraham, in *Handbook of Graphs and Networks*, edited by S. Bornholdt and H. G. Schuster (Wiley-VCH, Weinheim) (2003), P. 85.
- [42] J. Kleinberg, Nature **406**, 845 (2000).
- [43] S. Jespersen and A. Blumen, Phys. Rev. E **62**, 6270 (2000).
- [44] P. Sen and B. K. Chakrabarti, J. Phys. A **34**, 7749 (2001).
- [45] C. F. Moukarzel and M. A. de Menezes, Phys. Rev. E **65**, 056709 (2002).
- [46] P. Sen, K. Banerjee and T. Biswas, Phys. Rev. E **66**, 037102 (2002).
- [47] YuF. Chang, L. Sun and X. Cai, Phys. Rev. E **76**, 021101 (2007).
- [48] D. Li, G. Li, K. Kosmidis, H. E. Stanley, A. Bunde and S. Havlin, Europhys. Lett. **93**, 68004 (2011).
- [49] D. Stauffer and A. Aharony, *Introduction to Percolation Theory* (Taylor and Francis, 1991).